RESEARCH ARTICLE

Insights into the origins of inverted circular dichroism in thin films of a chiral side chain polyfluorene

Louis Minion[1,2,3] | Jessica Wade[1,2] | Juan Manuel Moreno-Naranjo[2,4] | Seán Ryan[4] | Giuliano Siligardi[3] | Matthew J. Fuchter[2,4]

[1]Department of Materials, Imperial College London, London, UK

[2]Centre for Processable Electronics, Imperial College London, South Kensington Campus, London, UK

[3]B23 Beamline, Diamond Light Source Ltd, Harwell Science and Innovation Campus, Didcot, UK

[4]Department of Chemistry and Molecular Sciences Research Hub, Imperial College London, White City Campus, London, UK

Correspondence

Matthew J. Fuchter, Department of Chemistry and Molecular Sciences Research Hub, Imperial College London, White City Campus, 82 Wood Lane, London W12 0BZ, UK.
Email: m.fuchter@imperial.ac.uk

Abstract

We synthesized a fluorene-bithiophene co-polymer with chiral side chains (**cPFT2**) and investigated its chiroptical properties via synchotronradiation circular dichroism. We observed that thin films of the polymer display an intense circular dichroism (CD) upon annealing, which is of opposite handedness to the CD reported for similar polyfluorenes bearing the same enantiomeric chiral side chain. We then contrast the properties of this polymer with chiral side chain fluorene homopolymer (**cPF**) and observe large differences in their thin film morphology. Using photoluminescence spectroscopy, we uncover evidence of polymer chain bending in **cPFT2**, which is further supported by theoretical calculations, and propose an explanation for the observed inverted optical activity.

KEYWORDS

circular dichroism, conjugated polymer, copolymers, optical activity, polyfluorene, polythiophene

---

Abbreviations: AFM, Atomic Force Microscopy; CD, circular dichroism; F8T2, poly(9,9-dioctylfluorene-alt-bithiophene); PFO, poly (9,9-dioctylfluorene); PL, photoluminescence.

1 | INTRODUCTION

To accelerate and realize the application of conjugated organic polymers in real-world technologies it is critical to understand and optimize their optical and electronic properties. Recently, molecular chirality has emerged as a strategy to impart new functionality into the active layers of optoelectronic devices. Optically active chiral materials will find application in high-efficiency displays and circularly selective photodetectors, while the chiral organization of conjugated organic molecules can give rise to spin-selective charge transport due to the chirality-induced spin selectivity effect.[1–3]

Several strategies have emerged to introduce chirality into polymer thin films, including the incorporation of chiral side chains, the combination of achiral polymers with chiral small molecule additives, and the use of chiral solvents.[4–8] The molecular weight, processing conditions, and post-deposition treatments (e.g., thermal annealing, solvent vapor exposure) have been shown to play a critical role in determining the strength of the optical response.[9–12] While design rules are still emerging, polyfluorene derivatives have far outperformed other conjugated polymers.[13–17]

In particular, poly(9,9-dioctyl-fluorene-*alt*-bithiophene) (F8T2)—a polymer developed for organic light emitting diodes (OLEDs) and phototransistors[18,19]—has shown large chiroptical responses after aggregation in chiral solvents (e.g., limonene[20]) and on blending with chiral small molecules (e.g., aza[6]helicene[21–24]). The precise molecular packing that gives rise to the giant chiroptical response in chiral phases of F8T2 is not well understood, which is surprising given the range of helical conformations that have been previously attributed to chiral side chain polythiophenes.[25,26]

Here, we use side chain engineering to introduce chirality into an F8T2 analog (cPFT2, Figure 1). While similar chemical structures have been considered in the literature, thin film fabrication has not been optimized and their optical response not carefully scrutinized.[5,21,27,28] For example, annealed thin films of chiral side chain polymers containing fluorene and thiophene

units display a positive bisignate cotton effect,[21,27] which is surprising given the handedness of the enantiopure side chains employed in these studies (e.g., (S)). With a fixed chiral side chain ((S)-3,7-dimethyloctyl), we contrast the optical activity of cPFT2 with the well-studied homopolymer chiral side chain polyfluorene (cPF). The two polymers display opposite sign bisignate CD spectra. Atomic force microscopy reveals that annealed thin films of the two polymers adopt a strikingly different morphology: the surface of cPF comprises a dense network of short, twisted fibril-like structures, while cPFT2 contains an assembly of smooth, curved, connected domains. Our results indicate that chiral aggregation of conjugated polymers is not only determined by the handedness of the chiral side chain (or chiral small molecule additive additive) but also depends on the conjugation length and torsional flexibility of the main chain. Uncovering the origin of these differences is vital for understanding and exploiting structure–property relationships in chiral polymer systems.

2 | MATERIALS AND METHODS

2.1 | Chemicals and synthesis

Details of the synthesis of cPF have been provided elsewhere.[22] To prepare cPFT2, 2,7-bis(4,4,5,5-tetramethyl-1,3,2-dioxaborolan-2-yl)-9,9-bis[(3S)-3, 7-dimethyloctyl]-9H-fluorene (cF8Bpin, 482 mg, 0.69 mmol, 1.00 equiv), 5,5′-dibromo-2,2′-bithiophene (224 mg, 0.69 mmol, 1.0 equiv), Pd(PPh$_3$)$_4$ (tetrakis(triphenylphosphine)-palladium(0), 12 mg, 0.01 mmol, 0.015 equiv) and aliquote (trioctylmethylammonium chloride, 15 mg) were added to a 25mL two-neck round bottomed flask with a stirrer bar and reflux condenser and placed under a nitrogen atmosphere. Nitrogen-purged 2M NaOH (sodium hydroxide, 3 mL) and toluene (15 mL) were added to the reaction vessel and the mixture was subjected to three freeze-pump-thaw cycles. After 60 h, a solution of cF8Bpin (48 mg, 0.07 mmol, 0.10 equiv) and Pd(PPh$_3$)$_4$ (1.2 mg, 0.001 mmol, 0.001 equiv) in toluene (2 mL) was deoxygenated by sparging with nitrogen for 10 min and added to the reaction mixture. After an additional 4 h at 100°C, a solution of PhI (iodobenzene, 0.5 mL) and Pd(PPh$_3$)$_4$ (1.2 mg) in toluene (2 mL) was deoxygenated by sparging with nitrogen for 10 min and added to the reaction mixture. After an additional 4 h at 100°C, the reaction was allowed to cool to room temperature and diethyldithiocarbamate trihydrate (1.0 g) was added and allowed to stir for 30 min. The reaction mixture was then poured into water and extracted twice with dichloromethane (CH$_2$Cl$_2$, 150 mL). The combined organic phase was dried over MgSO$_4$, filtered and reduced in volume to
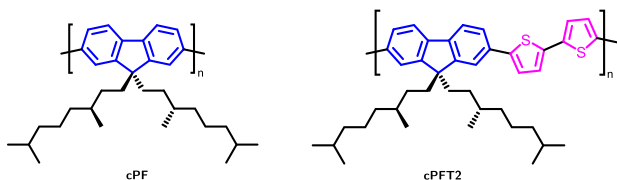
Chiral side chain polymers:

FIGURE 1 Two chiral polyfluorene analogs were investigated, cPF and cPFT2, with chemical structures shown here.

approx. 10 mL, and then added dropwise to cold methanol (200 mL) under vigorous stirring. The precipitate was filtered through a cellulose thimble and purified by successive Soxhlet extractions with methanol, acetone and ethyl acetate. The residue was then extracted with chloroform and concentrated to approx. 5 mL and then added dropwise to cold methanol (200 mL) under vigorous stirring. The precipitate was then collected by filtration and dried in air and under high vacuum overnight to afford the product as an orange solid (201 mg; GPC: $M_n = 33.8k$, $M_w = 74.4k$, $PDI = 2.2$).

2.2 | Preparation of films

cPFT2 and cPF were dissolved in toluene at a concentration of 30 mg/mL. Fused-silica substrates were cleaned in an ultrasonic bath using acetone and isopropyl alcohol for 10 min each. They were then transferred to an oxygen plasma asher for 3 min at 80 W immediately prior to spin-coating. Thin films were spin-coated using a static dispense method at 1500 rpm for 60 s, using a Laurell WS-650MZ-23NPP spin coater. Thermal annealing was performed in a nitrogen glovebox, with <0.1 ppm H_2O and O_2, for 10 min at 140°C.

2.3 | Characterization

CD spectra were measured using a Chirascan V100 spectrometer. Temperature-dependent CD spectroscopy and Mueller matrix polarimetry were measured in transmission mode at the B23 beamline at the Diamond Light Source. In situ, temperature-dependent spectra were obtained using a Linkam temperature-controlled stage with nitrogen. The heating/cooling rate was 10°C/min and the thin films were held at a given temperature for 1 min prior to CD/MMP measurements. CD peaks for the spectra at each temperature were found via the find peaks algorithm in the scipy package for the python programming language.[29] Photoluminescence was measured using an Edinburgh Instruments FLS 1000 spectrometer. Cross-polarized microscopy was performed using a BX50 Olympus polarizing microscope. Atomic Force Microscopy was measured using an Asylum Instruments MFP-3D in tapping mode. AFM images were processed using Gwyddion.[30] Roughness parameters reported were calculated via Gwyddion and are the RMS (S_q) parameter.

Film thicknesses were measured using a Dektak 3 profilometer by scratching the film and taking the mean of three measurements. DFT calculations were carried out using Gaussian 09 at the CAM-B3LYP/6-311G(d,p) level of theory.[31–34]

3 | RESULTS AND DISCUSSION

We have synthesized cPF and cPFT2 polymers using (S)-3,7-dimethyloctyl groups as chiral side chains for 9,9′-disubstituted fluorene. Chiral polyfluorenes with these types of side chain have been previously shown to display giant chiroptical properties.[5,14,15] For polyfluorene copolymers, it has previously been shown that the strongest chiroptical responses are generated when enantiopure side chains are attached to fluorene unit, with the size of the comonomer unit (torsional flexibility of the main chain) influencing the likelihood to form a chiral phase.[35] We studied the photophysical and chiroptical properties of cPFT2 in solution (Figure S1) and thin films (Figure 2) via UV/vis and CD spectroscopy. cPFT2 demonstrates spectral features reminiscent of achiral F8T2.[36] Both cPF and cPFT2 are CD silent in solution and demonstrate a weak optical activity in as-cast films (Figure 2). Thermal annealing at 140°C results in a considerable chiroptical response, generating a pronounced bisignate Cotton effect that persists on cooling to room temperature, with maximum g_{abs} of approximately 0.4 (500 nm) for cPFT2 and −0.7 (410 nm) for cPF (Figure S2). This is smaller than the g_{abs} reported by our group for F8T2 blended with aza[6]helicene (1.3).[22,23] Interestingly, the sign of the CD is opposite for cPF and cPFT2, despite having the same handedness of chiral side chain, with cPF demonstrating an intense negative band at high wavelengths and a positive band at lower wavelengths, and cPFT2 the opposite. Notably, the sign of CD observed for cPFT2 resembles the CD spectra we previously reported in films of achiral F8T2 blended with P-aza[6]helicene, while the CD observed for cPF here resembles the CD spectrum reported for achiral PFO blended with M-aza[6]helicene.[22,24] This indicates that the chiral side chains have the opposite effect on the chiroptical response of cPF and cPFT2, which indicates differences in their supramolecular assembly and backbone conformation.

For cPFT2, the sign of the CD inverts upon annealing—the weak CD of the lowest energy transition in as-cast cPFT2 (see inset of Figure 2) is negative, while the strong CD of the lowest energy transition in annealed cPFT2 is positive. A similar effect has been observed previously in chiral polyfluorenes, having been associated with the adoption of long-range chiral order upon annealing.[15] The line-shape of the low energy transition in cPFT2 also changes: The as-cast cPFT2 film exhibits strong absorption in the 350 – 500 nm region with a peak at ≈448 nm and a red-shifted shoulder at ≈475 nm, while the annealed thin films show a large decrease in overall absorption intensity and intense CD in the long wavelength shoulder.
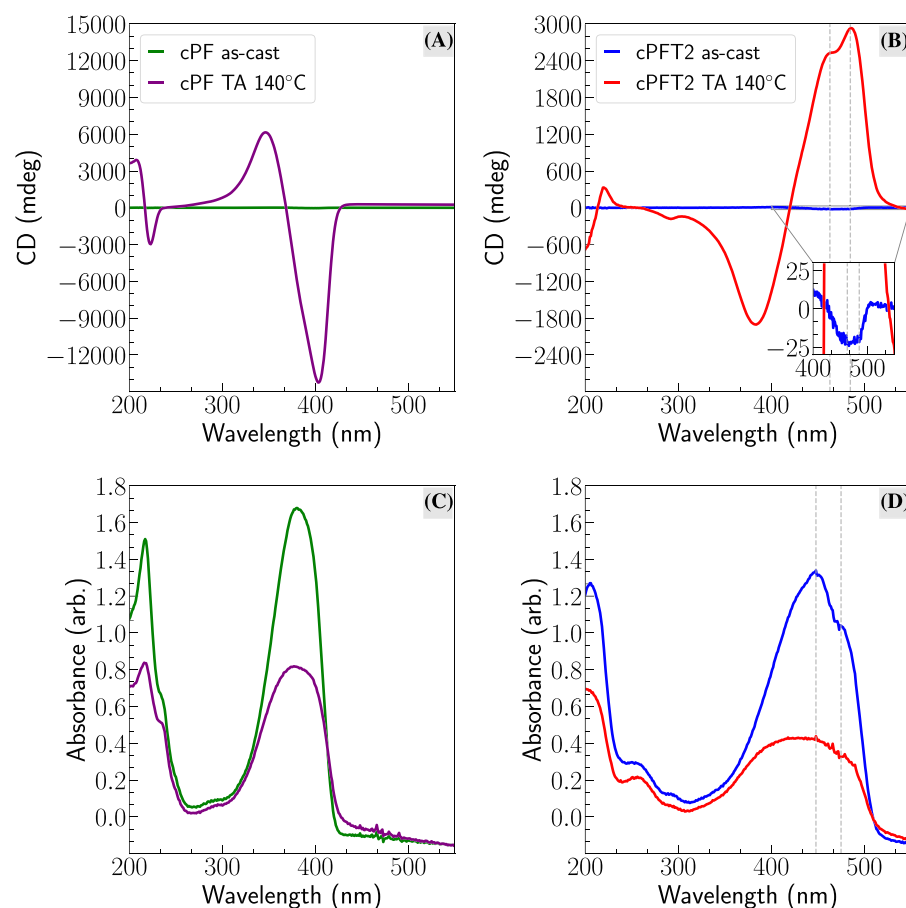
FIGURE 2 CD and absorption spectroscopy of annealed and as-cast chiral side chain polymer films. (A) CD and (C) absorption spectra of as-cast and annealed cPF, and (B) CD and (D) absorption spectra of as-cast and annealed cPFT2. Dashed lines indicate the positions of vibronic features.

Previous studies of the achiral analog polymer F8T2 noted the appearance of an intense red-shifted peak at ≈ 517 nm corresponding to the 0–0 vibronic peak upon annealing, attributed to the formation of tight J-aggregate type structures with long range order.[36] The absence of this peak at 517 nm in the absorption spectra indicates that chiral J-aggregate type structures are not present in cPFT2 thin films. This is evidence that the dimethyloctyl side chains present on cPFT2 disrupt the usual aggregation behavior of F8T2.

The change in optical activity due to annealing was studied using temperature-dependent synchotron-radiation CD spectroscopy, shown in Figures 3 and S3–S8. The use of in situ CD offers insights into the self-assembly processes. Above a certain temperature (T_{onset}), both cPF and cPFT2 show a rapid increase in CD, until a maximum temperature (T_{max}) after which the CD intensity decreases. T_{onset} and T_{max} for cPFT2 are slightly higher than cPF (T_{onset} cPF $\approx 80°$C and cPFT2 $\approx 100°$C, T_{max} cPF $\approx 130°$C, and cPFT2 $\approx 160°$C) (Figure 3). We note that the T_{onset} for cPFT2 observed roughly corresponds to the glass transition temperature measured by Joseph et al using DSC,[21] and T_{max} to the temperature of a peak in the DSC thermogram that the authors

attributed to an irreversible phase transition to a more thermodynamically stable state than the kinetically stable as-cast film. This indicates that in order to induce the formation of a chiral phase, heating above the glass transition is required. At higher temperatures around T_{max}, CD spectra of cPFT2 lose their bisignate line-shape, and display a long wavelength shoulder. (Figure 3). Notably, this is the opposite to the behavior observed in films thermally annealed at 140°C and immediately quenched (Figure 2). The line-shape does not recover upon cooling, but the magnitude of CD does. Further experiments are required to uncover the origin of this change, but it may be associated with the phase transition at a similar temperature observed by Joseph et al.[21] We also examined the change in absorption as a function of temperature in cPFT2 (Figures S6 and S8) and cPF (Figures S3 and S4). During heating, the absorption intensity for both polymers significantly decreases with loss of the vibronic fine structure. The decrease of absorption intensity and broadening have been associated with a rearrangement of polymer backbones and increased chain coiling.[9,27,37,38]

Photoluminescence (PL) spectra were acquired of as-cast and annealed films of cPFT2 (Figure 4). The PL spectra include vibronic structure, with strong emission from

FIGURE 3 Results of in situ CD spectroscopy during heating and cooling of the two polymers under N_2. Dashed vertical lines in (B) and (D) indicate T_{max} and T_{onset} (see main text). (A) In situ CD spectra of a 98 nm thick cPFT2 film (20–200°C). Spectra acquired during the cooling cycle are included in the Supporting Information. (B) Peak CD of each spectrum versus temperature, for both the heating and cooling of the cPFT2 film. (C) In situ CD spectra of a 133 nm thick cPF film (20–200°C). (D) Peak CD of each spectrum versus temperature, for both the heating and cooling of the cPF film.
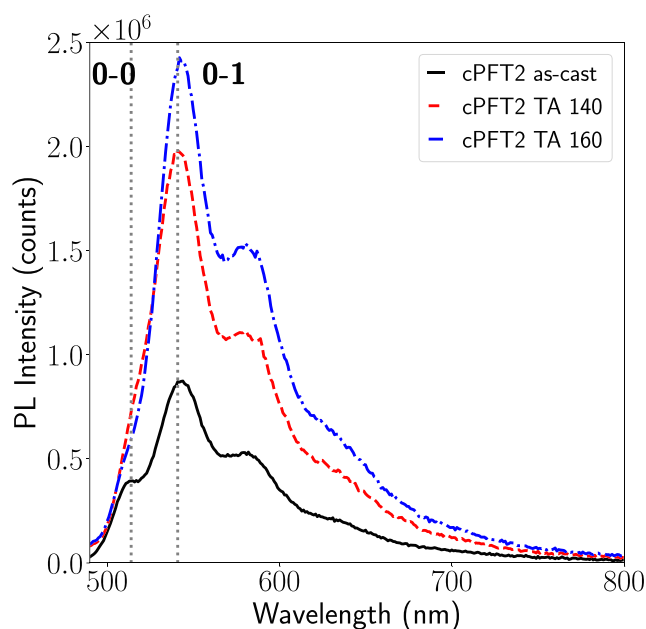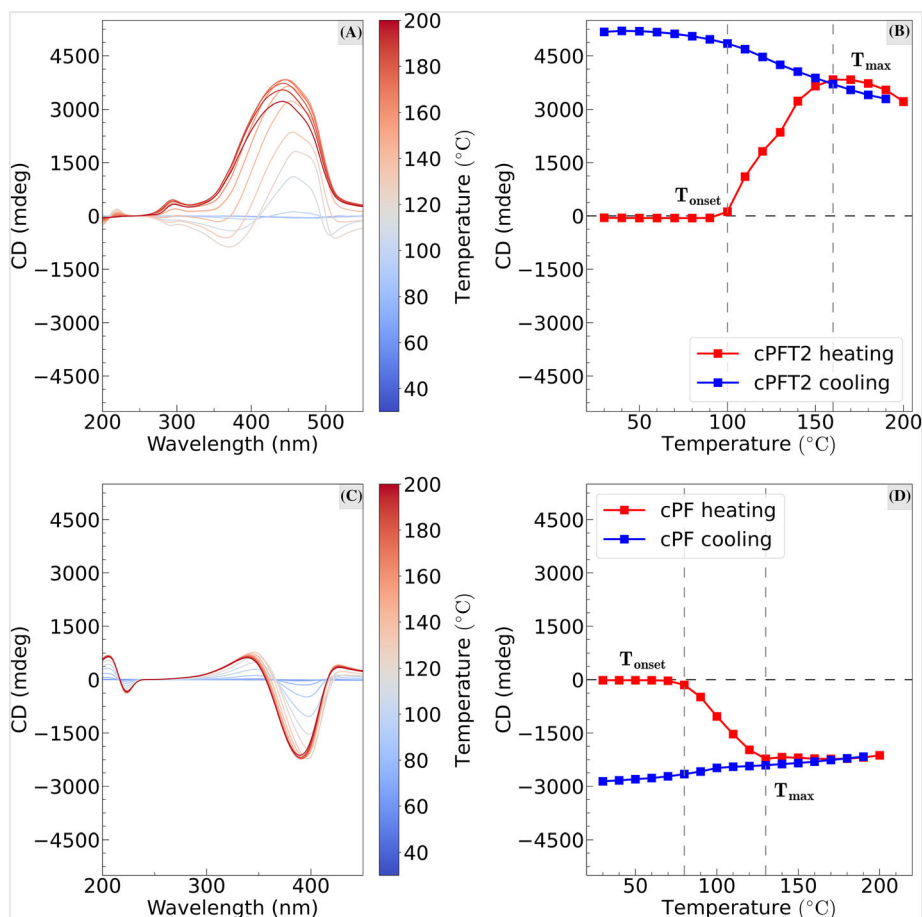

the 0-1 peak ($\lambda = 540$ nm), and a weak 0-0 shoulder ($\lambda = 514$ nm). Upon annealing, the 0–0 peak decreases relative to the 0-1 peak (Figure S9), which we explore in further detail in the Supporting Information. Hestand and Spano have shown PL is particularly sensitive to chain-bending in conjugated polymers, and that chain bending is associated with with a decreased intensity of the 0–0 emission peak relative to the 0–1 peak.[39,40] The line-shape of the PL spectra indicate that annealing cPFT2 increases backbone bending. A bent chromophore structure with *syn* thiophenes pointing inwards, and side chains pointing outwards, known as a helical cisoid, has been proposed as the origin of spectral features in achiral F8T2 aggregates and associated with the formation of single chain helices in other polythiophenes.[40,41] The assembly of cPFT2 chains into helical cisoid type structures via the in-plane bending of the main backbone, with a handedness determined by the chiral side chain, may explain the difference in observed CD. Compared with cPF, this may be possible in cPFT2 due to greater conformational flexibility afforded by the more freely

FIGURE 4 Photoluminescence spectra of cPFT2 films, as-cast and annealed at 140°C and 160°C.

moving thiophene units and larger spacing between sterically hindering side chains. This theory is further supported by DFT calculations discussed below.

To further explore the origins of this chiroptical response, we used Mueller matrix polarimetry, which can discriminate between circular and linear contributions to the optical response (Figures S10 and S11). Logarithmic decomposition of the spectra of the homogeneously depolarizing film[42] shows very small linear dichroism and birefringence, showing that the large CD observed is not apparent CD originating from the coupling of linear dichroism and birefringence.[10,43–45]

Atomic Force Microscopy (AFM) provides information on the morphology and surface topography of the as-cast and annealed films (Figure 5). Calculation of roughness parameters for each image (Table 1) shows that annealing increases the surface roughness for both cPF and cPFT2. The as-cast cPF film is smooth and featureless, with small twisted fibrils (300 nm long and 20 nm wide) that appear after annealing. Similar fibril-like structures are also present in the as-cast cPFT2 films and extend into curved, connected domains upon annealing. The large differences in morphology support the theory that the thiophene units afford greater torsional flexibility in the backbone of cPFT2, which leads to a significantly different polymer microstructure after annealing. Polarized optical microscopy reveals that annealed films of both polymers comprise of micron sized crystalline domains, with cPFT2 showing larger, smoother domains with a more distinct texture.

Theoretical calculations with density functional theory at the CAM-B3LYP/6-311G(d,p) level for cPFT2 and cPF were performed using Gaussian 09 to gain insight into the molecular geometry of the backbone with and without the thiophene units, and the influence of the chiral side chain upon preferred conformation. As shown in Figure 6, a scan of the potential energy surface versus the dihedral angle between adjacent monomer units (θ) indicates differences in the preferred conformations of cPF and cPFT2 backbones. Energy minima at approximately $\theta = 135°$ appear in both systems, however interestingly, dihedral angles which place the (S)-3,7-dimethyloctyl side chains in a $syn (\theta = 0°)$ or $anti (\theta = 180°)$ conformation appear as energy maxima in the simulation of cPF, and as energy minima in cPFT2. These predictions indicate that cPFT2 polymer chains have a greater degree of

TABLE 1 Roughess parameters.

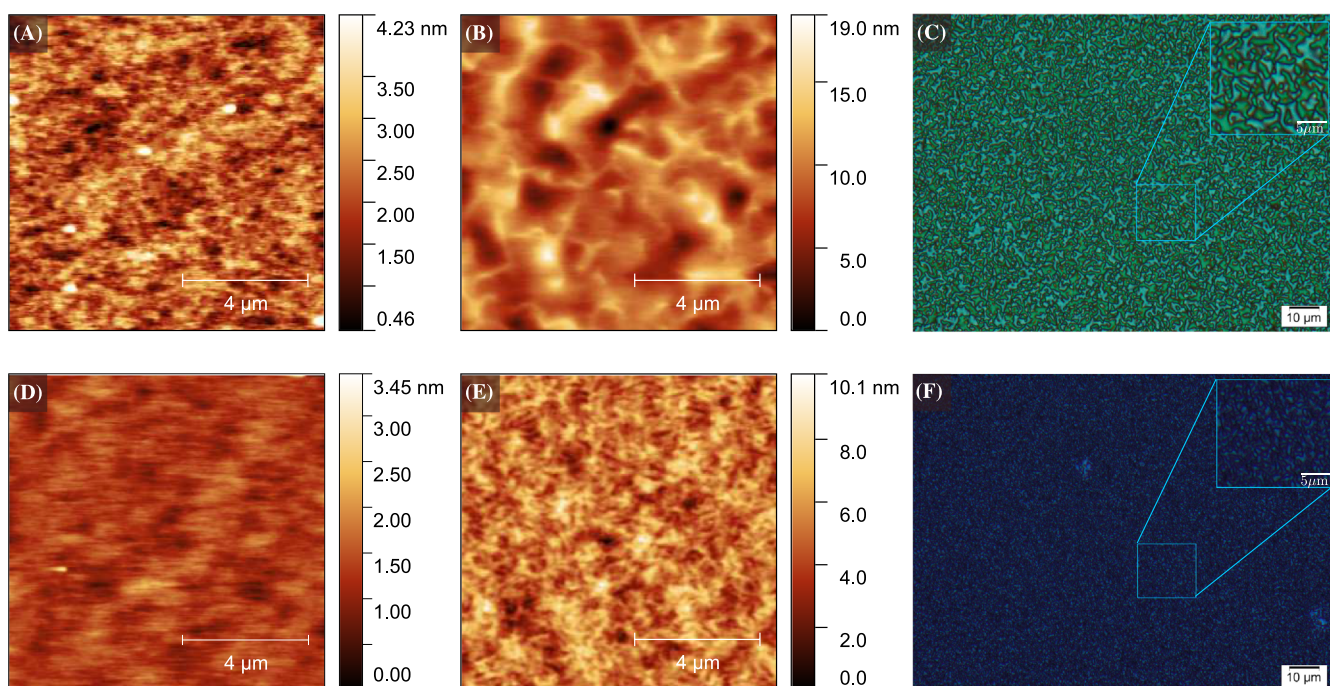| Sample	RMS roughness (nm)
cPF as-cast	0.23
cPF (annealed)	1.20
cPFT2 as-cast	0.59
cPFT2 (annealed)	2.40

FIGURE 5 (A) AFM image of as-cast cPFT2. (B) AFM image of annealed cPFT2. (C) Cross-polarized microscope image of annealed cPFT2. (D) AFM image of as-cast cPF. (E) AFM image of annealed cPF. (F) Cross polarized microscope image of annealed cPF.
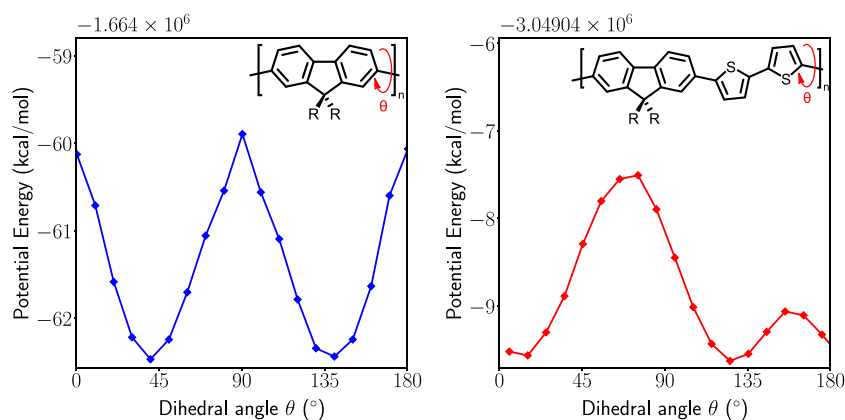
FIGURE 6 (R = *S*-3,7-dimethyloctyl) Relaxed potential energy scan of cPF and cPFT2 dimers. Dimers consisting of two of the repeating units in cPF and cPFT2, with the main chains capped by Me groups, were constructed using Gaussview, then the structure optimized using Gaussian 09 at the CAM-B3LYP/6-311G(d,p) level of theory. The dihedral angle highlighted with a red arrow on each diagram was changed, then the structure optimized again, keeping the dihedral angle fixed at this new angle. The process was repeated to scan the potential energy surface as a function of dihedral angle. The full side chain was included in the model.
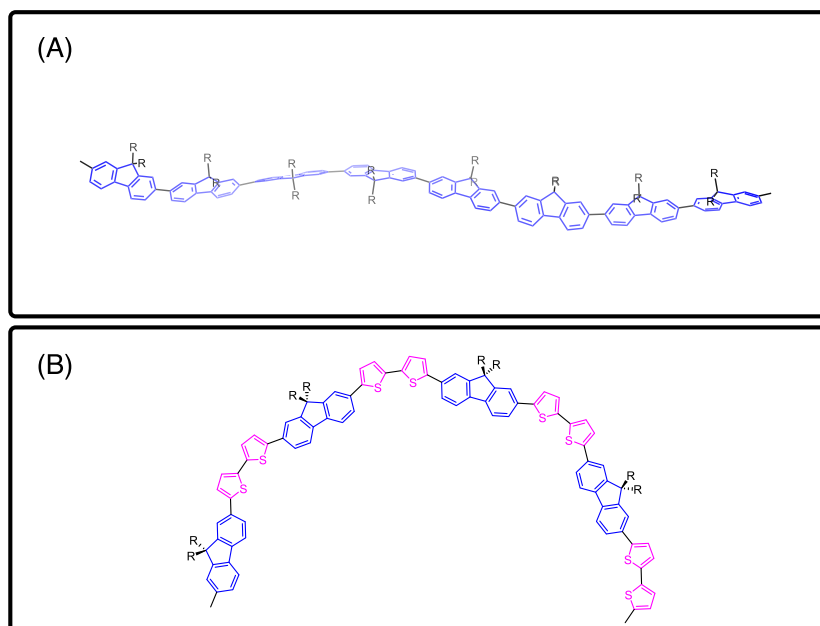

FIGURE 7 Cartoons representing potential polymer backbone conformations. (A) A straight main chain conformation, with a ribbon-like twist along it. (B) The "bent" chromophore arrangement, in which the backbone adopts a coil-like structure. We propose that cPF adopts a configuration like (A), while cPFT2 adopts the structure like (B).

planarity compared to cPF, and are stable with aliphatic side chains in a *syn* conformation, which when combined with the discussion of PL evidence above supports the proposal that cPFT2 chains adopt a bent-chromophore type conformation upon annealing. This is contrasted with cPF, where the results show that such a backbone conformation would be strongly disfavored, with the polymer instead favoring the adoption of a straight main chain. These conformations are illustrated in Figure 7.

4 | CONCLUSION

The chiroptical properties of chiral side chain polyfluorenes depend on the chemical structure of polymer backbone. We have compared the chiroptical properties and morphology of cPFT2 and cPF and identified a possible origin of the opposite sign CD. AFM reveals large differences in the self-assembly processes of the two polymers. Comparison with the CD line-shapes associated with

chiral induction in F8T2 via other methods indicate that the *S*-enantiomer side chains induce chirality in the polymer backbone in the opposite manner to which they do in cPF and other chiral polyfluorenes with shorter monomers. For example, previously reported blends of F8T2 with *P*-aza[6]helicene match the sign of CD observed for cPFT2, while blends of PFO with *M*-aza[6] helicene match that observed for cPF.[22] However, the $|g_{abs}|$ of cPFT2 is not as large as is observed in F8T2:aza [6]helicene blends. Photoluminescence studies indicate a degree of chain-bending upon annealing providing evidence that suggests the adoption of a helical-cisoid type polymer conformation, with outward facing chiral side chains influencing the turn direction. This is contrasted to cPF, in which tighter steric requirements restrict polymer flexibility and enforce a larger degree of nonplanarity, preventing coiling and leading to a different supramolecular structure. Further work is needed to understand the morphology of chiral side chain polyfluorenes and annealing induced changes in-depth, but these results show that simple rules following from the enantiomer of side chain on a polymer backbone cannot reliably be used to predict the sign of the chiropitcal response of CD in thin films.

DATA AVAILABILITY STATEMENT
Data are available upon request.

ORCID

Louis Minion https://orcid.org/0000-0003-0903-6686
Matthew J. Fuchter https://orcid.org/0000-0002-1767-7072

REFERENCES

1. Brandt JR, Salerno F, Fuchter MJ. The added value of small-molecule chirality in technological applications. *Nat Rev Chem*. 2017;1(6):45.

2. Naaman R, Waldeck DH. Chiral-induced spin selectivity effect. *J Phys Chem Lett*. 2012;3(16):2178-2187.

3. Wan L, Shi X, Wade J, Campbell AJ, Fuchter MJ. Strongly circularly polarized crystalline and *β*-phase emission from poly (9,9-dioctylfluorene)-based deep-blue light-emitting diodes. *Adv Optical Mater*. 2021;9(19):2100066.

4. Lakhwani G, Meskers SCJ. Circular selective reflection of light proving cholesteric ordering in thin layers of chiral fluorene polymers. *J Phys Chem Lett*. 2011;2:1497-1501.

5. Oda M, Meskers SCJ, Nothofer HG, Scherf U, Neher D. Chiroptical properties of chiral-substituted polyfluorenes. *Synth Metals*. 2000;111:575-577.

6. Wan L, Wade J, Salerno F, et al. Inverting the handedness of circularly polarized luminescence from light-emitting polymers using film thickness. *ACS Nano*. 2019;13(7):8099-8105.

7. Wang L, Suzuki N, Liu J, et al. Limonene induced chiroptical generation and inversion during aggregation of achiral polyfluorene analogs: structure-dependence and mechanism. *Polym Chem*. 2014;5:5920-5927.

8. Yang Y, da Costa RC, Smilgies DM, Campbell AJ, Fuchter MJ. Induction of circularly polarized electroluminescence from an achiral light-emitting polymer via a chiral small-molecule dopant. *Adv Mater*. 2013;25(18):2624-2628.

9. Abbel R, Schenning APHJ, Meijer EW. Molecular weight optimum in the mesoscopic order of chiral fluorene (co)polymer films. *Macromolecules*. 2008;41(20):7497-7504.

10. Albano G, Pescitelli G, Di Bari L. Reciprocal and non-reciprocal chiroptical features in thin films of organic dyes. *ChemNanoMat*. 2022;8(8):e202200219.

11. Albano G, Salerno F, Portus L, Porzio W, Aronica LA, Di Bari L. Outstanding chiroptical features of thin films of chiral oligothiophenes. *ChemNanoMat*. 2018;4(10):1059-1070.

12. Zinna F, Albano G, Taddeucci A, et al. Emergent nonreciprocal circularly polarized emission from an organic thin film. *Adv Mater*. 2020;32(37):2002575.

13. Albano G, Pescitelli G, Di Bari L. Chiroptical properties in thin films of *π*-conjugated systems. *Chem Rev*. 2020;120(18):10145-10243.

14. Craig MR, Jonkheijm P, Meskers SCJ, Schenning APHJ, Meijer EW. The chiroptical properties of a thermally annealed film of chiral substituted polyfluorene depend on film thickness. *Adv Mater*. 2003;15(17):1435-1438.

15. Lakhwani G, Gielen J, Kemerink M, Christianen PCM, Janssen RAJ, Meskers SCJ. Intensive chiroptical properties of chiral polyfluorenes associated with fibril formation. *J Phys Chem B*. 2009;113(43):14047-14051.

16. Nuzzo DD, Kulkarni C, Zhao B, et al. High circular polarization of electroluminescence achieved via self-assembly of a light-emitting chiral conjugated polymer into multidomain cholesteric films. *ACS Nano*. 2017;11(12):12713-12722.

17. Wang K, Xiao Y. Chirality in polythiophenes: a review. *Chirality*. 2021;33(8):424-446.

18. Levermore PA, Jin R, Wang X, de Mello JC, Bradley DDC. Organic light-emitting diodes based on poly(9,9-dioctylfluorene-co-bithiophene) (F8T2). *Adv Funct Mater*. 2009;19(6):950-957.

19. Wang X, Wasapinyokul K, De Tan W, Rawcliffe R, Campbell AJ, Bradley DDC. Device physics of highly sensitive thin film polyfluorene copolymer organic phototransistors. *J Appl Phys*. 2010;107(2):24509.

20. Kawagoe Y, Fujiki M, Nakano Y. Limonene magic: noncovalent molecular chirality transfer leading to ambidextrous circularly polarised luminescent π-conjugated polymers. *New J Chem*. 2010;34(4):637.

21. Joseph JP, Abraham SR, Dutta A, Baev A, Swihart MT, Prasad PN. Modulating the chiroptical response of chiral polymers with extended conjugation within the structural building blocks. *J Phys Chem Lett*. 2022;13(39):9085-9095.

22. Wade J, Hilfiker JN, Brandt JR, et al. Natural optical activity as the origin of the large chiroptical properties in π-conjugated polymer thin films. *Nat Commun*. 2020;11:6137.

23. Wan L, Wade J, Wang X, Campbell AJ, Fuchter MJ. Engineering the sign of circularly polarized emission in achiral polymer-chiral small molecule blends as a function of blend ratio. *J Materials Chem C*. 2022;10(13):5168-5172.

24. Ward MD, Wade J, Shi X, Nelson J, Campbell AJ, Fuchter MJ. Highly selective high-speed circularly polarized photodiodes based on π-conjugated polymers. *Adv Optical Mater*. 2022;10: 2101044.

25. Ikai T, Takayama K, Wada Y, Minami S, Apiboon C, Shinohara K. Synthesis of a one-handed helical polythiophene: a new approach using an axially chiral bithiophene with a fixed syn-conformation. *Chem Sci*. 2019;10(18):4890-4895.

26. Langeveld-Voss BMW, Janssen RAJ, Meijer EW. On the origin of optical activity in polythiophenes. *J Molec Struct*. 2000; 521(1-3):285-301.

27. Cho MJ, Ahn J-S, Kim Y-U, et al. New fluorene-based chiral copolymers with unusually high optical activity in pristine and annealed thin films. *RSC Adv*. 2016;6(28):23879-23886.

28. Sub Oh H, Liu S, Jee H, Baev A, Swihart MT, Prasad PN. Chiral poly(fluorene-alt-benzothiadiazole) (PFBT) and nanocomposites with gold nanoparticles: plasmonically and structurally enhanced chirality. *J Am Chem Soc*. 2010;132(49):17346-17348.

29. Virtanen P, Gommers R, Oliphant TE, et al. SciPy 1.0: fundamental algorithms for scientific computing in Python. *Nat Methods*. 2020;17(3):261-272.

30. Nečas D, Klapetek P. Gwyddion: an open-source software for SPM data analysis. *Open Phys*. 2012;10(1):181-188.

31. Frisch MJ, Trucks GW, Schlegel HB, et al. Gaussian 09 Revision C.01: Gaussian, Inc.; 2010.

32. Krishnan R, Binkley JS, Seeger R, Pople JA. Self-consistent molecular orbital methods. XX. A basis set for correlated wave functions. *J Chem Phys*. 1980;72(1):650-654.

33. McLean AD, Chandler GS. Contracted Gaussian basis sets for molecular calculations. I. Second row atoms, Z =11-18. *J Chem Phys*. 1980;72(10):5639-5648.

34. Yanai T, Tew DP, Handy NC. A new hybrid exchange-correlation functional using the Coulomb-attenuating method (CAM-B3LYP). *Chem Phys Lett*. 2004;393(1-3):51-57.

35. Kulkarni C, van Son MHC, Di Nuzzo D, Meskers SCJ, Palmans ARA, Meijer EW. Molecular design principles for achieving strong chiroptical properties of fluorene copolymers in thin films. *Chem Mater*. 2019;31(17):6633-6641.

36. Ma T, Wang Z, Song C, et al. J-aggregate behavior of poly[(9,-9-dioctyluorenyl-2,7-diyl)-alt-co-(bithiophene)] (F8T2) in crystal and liquid crystal phases. *J Phys Chem C*. 2019;123(39): 24321-24327.

37. Barford W, Marcus M. Perspective: optical spectroscopy in π-conjugated polymers and how it can be used to determine multiscale polymer structures. *J Chem Phys*. 2017;146(13): 130902.

38. Lee GJ, Choi EH, Ham WK, Hwangbo CK, Cho MJ, Choi DH. Circular dichroism, surface-enhanced raman scattering, and spectroscopic ellipsometry studies of chiral polyfluorene-phenylene films. *Opt Mater Express*. 2016;6(3):767-781.

39. Hestand NJ, Spano FC. The effect of chain bending on the photophysical properties of conjugated polymers. *J Phys Chem B*. 2014;118(28):8352-8363.

40. Wang L, Rothberg L. Complications in the interpretation of F8T2 spectra in terms of morphology. *J Phys Chem B*. 2021; 125(21):5660-5666. doi:10.1021/acs.jpcb.1c02701

41. Kiriy N, Jähne E, Adler H-J, et al. One-dimensional aggregation of regioregular polyalkylthiophenes. *Nano Lett*. 2003;3(6): 707-712.

42. Arteaga O, Kahr B. Characterization of homogenous depolarizing media based on Mueller matrix differential decomposition. *Opt Lett*. 2013;38(7):1134.

43. Albano G, Lissia M, Pescitelli G, Aronica LA, Di Bari L. Chiroptical response inversion upon sample flipping in thin films of a chiral benzo[1,2-b:4,5-b']dithiophene-based oligothiophene. *Mater Chem Front*. 2017;1:2047-2056.

44. Salij A, Goldsmith RH, Tempelaar R. Theory of apparent circular dichroism reveals the origin of inverted and noninverted chiroptical response under sample flipping. *J Am Chem Soc*. 2021;143:21519-21531. doi:10.1021/jacs. 1c06752

45. Wolffs M, George SJ, Tomovic Z, Meskers SCJ, Schenning APHJ, Meijer EW. Macroscopic origin of circular dichroism effects by alignment of self-assembled fibers in solution. *Angewandte Chemie Int Ed*. 2007;46(43):8203-8205.

SUPPORTING INFORMATION

Additional supporting information can be found online in the Supporting Information section at the end of this article.